北海道大学工学部研究報告
第171号（平成6年）

Bulletin of the Faculty of Engineering
Hokkaido University, No. 171 (1994)

Shear Resisting Model of Reinforced and Prestressed Concrete Beams Based on Finite Element Analysis

Yasuhiko SATO, Tamon UEDA and Yoshio KAKUTA

(Received June 30, 1994)

Abstract

In this study a shear resisting model was developed by non-linear finite element analysis. Concrete strength, the shear span to effective depth ratio, stiffness of main and web reinforcement, yielding of web reinforcement and prestressing force were chosen as parameters. The shear resisting model was defined as summation of shear resisting forces by concrete in a compression zone, by web reinforcement and others in a shear cracking zone, and by concrete in a horizontal zone linking the compressive and shear cracking zones. This model can be applied to reinforced and prestressed concrete beams reinforced with steel bars and/or FRP (Fiber Reinforced Plastic) rods.

1. Introduction

Recently, it has been desirable to construct concrete structures which have good durability as well as high structural performance. Therefore there are many studies in field of durability, such as studies on cathodic protection[1]. From these circumstances, considerable interest is being shown in replacing steel with FRP rods which have excellent anticorrosion resistance and many studies have been conducted. As a results the basic characteristics of concrete members using FRP rods are clarified. It is now desirable to provide a design code applicable to both the concrete members with FRP rods and those with ordinary reinforcement.

The authors clarified how mechanical properties of reinforcement such as Young's modulus and yield strength influence the ultimate shear strength as well as the shear resisting behavior[2]. In this paper, a numerical study using nonlinear finite element analysis was carried out in order to develop a shear resisting model for reinforced and prestressed concrete beams with web reinforcement using not only FRP rods but also steel.

In this study, at first, the shear resisting model for reinforced and prestressed concrete beams in which shear reinforcement does not yield is proposed. Secondly, the shear resisting model for reinforced and prestressed concrete beams in which web reinforcement yields is proposed.

Dept. of Civile Engineering, Faculty of Engineering, Hokkaido University, Sapporo 060 Japan

2. Outline of Analysis

2.1 Finite Element Program

The nonlinear finite element program in this study was developed for two dimensional analysis of linear members[3].

2.2 Analytical Specimen

Figure 1 shows the finite element meshes in this study. They are simply supported beams subjected to two-point monotonic loading. In the analysis enforced displacements are given at the loading point and prestressing forces are applied as a load at a node of steel element attached to specimen.

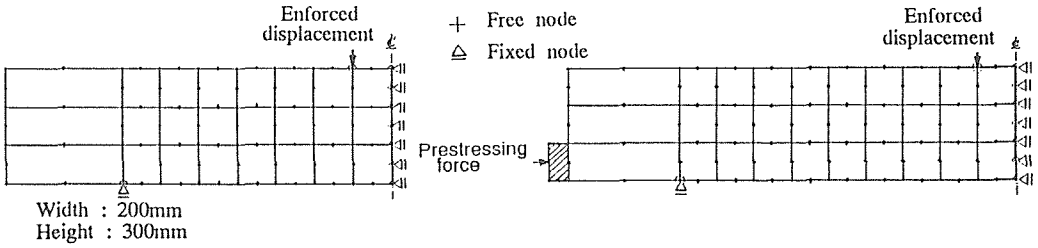

Fig. 1 Finite Element Meshes

2.3 Analytical Parameters

The following six parameters were chosen in the numerical study.

(1)Concrete strength (f'_c=20, 29, 44 MPa)

(2)Shear span to effective depth ratio (a/d=1.6, 2.0, 2.4, 3.2)

(3)Stiffness of main reinforcement (p_sE_s=1236, 2472, 4944, 7416 MPa)

(4)Stiffness of web reinforcement (p_wE_w=137, 412, 824, 1235 MPa)

(5)Prestressing force (P_{eff}=78~470 kN)

(6)Yielding of web reinforcement

where p_s: main reinforcement ratio, p_w: web reinforcement ratio, E_s: Young's modulus of main reinforcement, and E_w: Young's modulus of web reinforcement.

It is generally known that the size of loading plate influences to shear strength of deep beams[4]. But this effect is not taken into account in this study. Effect of compressive reinforcement is not considered either.

2.4 Failure Mode in Analysis

In the computed results of FEM, softening of concrete around loading point was observed at peak load. It can be said that the failure mode is shear compressive failure. So the proposed shear resisting model developed by the numerical study using FEM should be applied to the shear compressive failure in which crushing occurs at concrete around loading point in a beam but not shear tension failure.

3. Shear Resisting Model in The Case Where Web Reinforcement Does Not Yield

3.1 Shear Resisting Model

At a cracked section, the internal shear resisting forces are a shear force carried by concrete at the compression zone and shear forces at the shear cracking zone (see Fig. 2). In this paper the equilibrium of shear forces is assumed as follows.

$$V = V_{cpz} + V_{dcz} \tag{1}$$

where V_{cpz} is the shear resisting force at the compression zone which is above by a neutral axis, and V_{dcz} is defined as summation of the shear resisting force, V_{web} by web reinforcement and V_{str}, by others.

$$V = V_{cpz} + V_{web} + V_{str} \tag{2}$$

Shear cracking zone is a path linking gauss points with crack angles. There are many shear cracking paths as shown in Fig. 3. But it was observed that the shear resisting force at a shear cracking path through the point at which the neutral axis line intersected with the straight line connecting the loading and supporting points is the largest. In this study, the failure section is assumed to consist of compression zone at loading point where crushing of concrete occurs and shear cracking zone where the shear resisting force is the largest and the horizontal zone linking this compression and shear cracking zones.

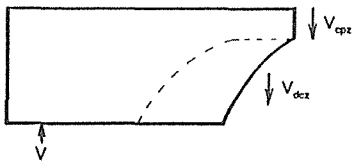

Fig. 2 Shear Resisting Model

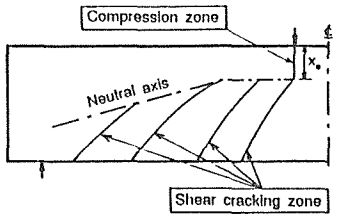

Fig. 3 Assumed Compression Zene and Shear Cracking Zene

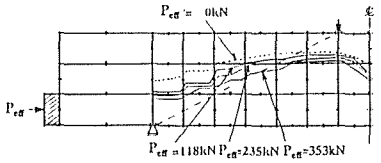

Fig. 5 Position of Neutral Axis of Prestressed Concrete Beams

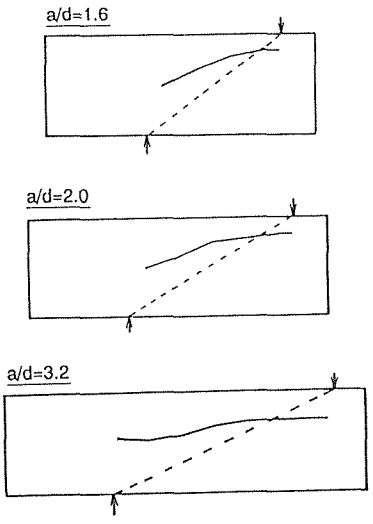

Fig. 4 Position of Neutral Axis of Reinforced Concrete Beams

Figure 4 shows the neutral axis lines in reinforced concrete beams for different a/d ratios. Figure 5 shows that the neutral axis lines in a prestressed concrete beam for different prestressing forces. It is observed that depth to the neutral axis starts to increase around the point where the neutral axis line intersects with the straight line connecting the loading and supporting points. Therefore the shear resisting zone which links the shear cracking and compression zones is assumed to be a horizontal line. The shear resisting model is thus assumed as follows (see Fig. 6).

$$V = V_{cpz} + V_{web} + V_{str} - V_{com} \tag{3}$$

where V_{cpz}: shear resisting force by concrete at the compression zone, V_{web}: shear resisting force by web reinforcement at the shear cracking zone, V_{str}: shear resisting force by other than web reinforcement at the shear cracking zone, and V_{com}: shear resisting force by concrete at the horizontal zone linking the compression and shear cracking zones.
Equation (3) can be rewritten as Eq. (4) because these resisting forces are calculated by integration of resisting stresses over the resisting zones (see Fig. 7).

$$V = bx_e\,\overline{\tau_{cpz}} + p_w bL_{web}\,\overline{\sigma_{web}} + bL_{str}\,\overline{\tau_{str}} - bL_{com}\,\overline{\sigma'_{com}} \tag{4}$$

where $\overline{\tau_{cpz}}$: average shear stress at the compression zone, $\overline{\sigma_{web}}$: average tensile stress of web reinforcement at the shear cracking zone, $\overline{\tau_{str}}$: average shear stress at the shear cracking zone, $\overline{\sigma'_{com}}$: average compressive stress at the horizontal zone, L_{web}: horizontal projected length of the shear cracking zone, L_{str}: vertical projected length of the shear cracking zone, L_{com}: length of the horizontal zone, x_e: depth of the compression zone, and b: beams width. Then L_{com} is calculated by the following equation.

$$L_{com} = \frac{a}{h} x_e \quad (a > h) \tag{5}$$

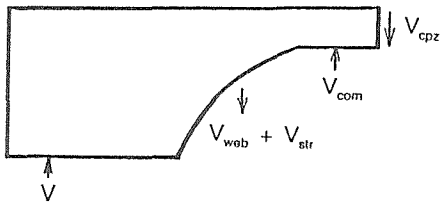

Fig. 6 Shear Resisting Model

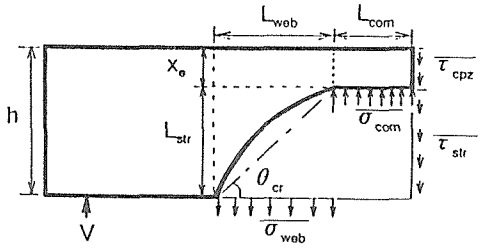

Fig. 7 Distribution of Shear Resisting Strsses

Figure 8 shows crack patterns of the analytical specimens. It is clearly seen that the shear cracking angles become smaller as the prestressing force increases. In this study the shear cracking angle θ_{cr} (See Fig. 7) is assumed as in the following equation which is a function of prestress level defined as the ratio of prestress to concrete strength.

$$\theta_{cr} = 45\left[1 - \left(\frac{\sigma_p}{f_c'}\right)^{0.7}\right] \qquad (deg) \tag{6}$$

where σ_P : prestressing force divided by the cross sectional area. As Eq.(6) indicates, the crack angle becomes 45 degree in the case of reinforced concrete beams.
The length L_{web} is calculated by the following equation.

$$L_{web}=\frac{L_{str}}{tan\ \theta_{cr}} \tag{7}$$

where $L_{str}=h-x_e$. The following equation should be satisfied because of geometric condition.

$$L_{com}+L_{web}<a \tag{8}$$

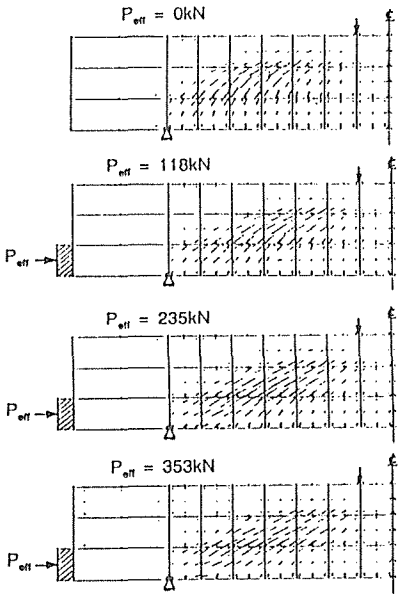

Fig. 8 Crack Pattern of Analytical Specimens

3. 2 Depth of Compression Zone

Figure 9 shows relationships between the depth of the compression zone, x_e divided by the value calculated by the bending theory shown in Eqs.(9) and (10) and the concrete strength in reinforced concrete beams.

$$x=kd \tag{9}$$

$$k=-np_s+\sqrt{(np_s)^2+2np_s} \tag{10}$$

It seems that the normalized depth, x_e/x is approximately the same for different concrete strengths. That is, the effect of concrete strength, in other words Young's modulus of concrete, can be eliminated by using the normalized depth. Normalized depth of compression zone becomes large as stiffness of main and web reinforcement increase as shown in Figs.10 and 11. Figure 12 shows relationships between normalized depth of the compression zone and a/d. The normalized depth of the compression zone becomes small as a/d decreases.

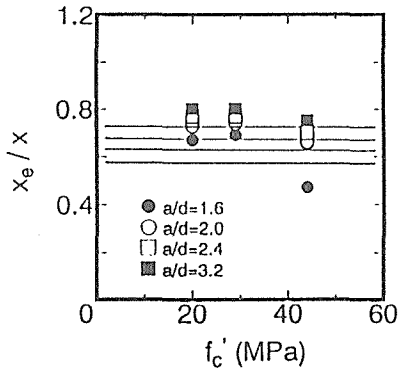

Fig. 9 Relationships between Size of Compression Zone and Concrete Strength

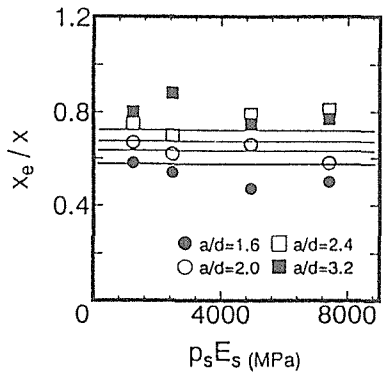

Fig. 10 Relationships between Size of Compression Zone and Stiffness of Main Reinforcement

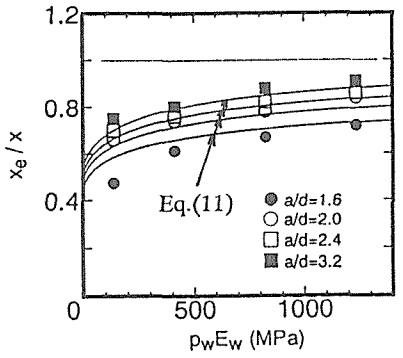

Fig. 11 Relationships between Size of Compressin Zone and Stiffness of Web Reinforcement

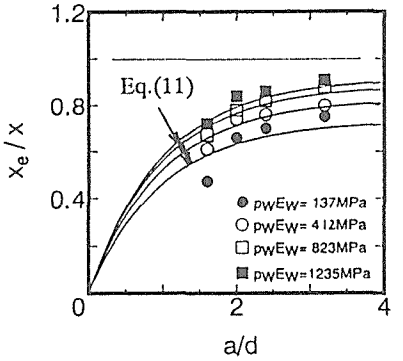

Fig. 12 Relationships between Size of Compressiom Zone and a/d

On the other hand, Fig.13 shows relationships between the depth of the compression zone divided by the value calculated by Eq.(9) and prestress level. The depth of the compression zone becomes larger than that of reinforced concrete beams as the prestress level increases.

In this study the following equation is assumed for prediction of the depth of the compression zone.

$$\frac{x_e}{x}=\frac{1-e^{-\left(\frac{a}{d}\right)}}{1+3.2^{-0.12(P_wE_w)^{0.4}}}\left[1+\left(\frac{\sigma_p}{f_c'}\right)^{0.7}\right] \tag{11}$$

Solid line in Figs.9 to 13 indicates the results predicted by Eq.(11). It is clearly seen that Eq. (11) can predict the analyzed results with reasonable accuracy.

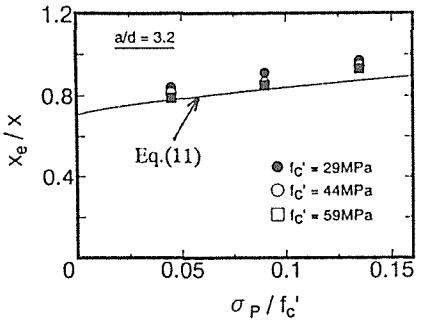

(a) For different concrete strengths

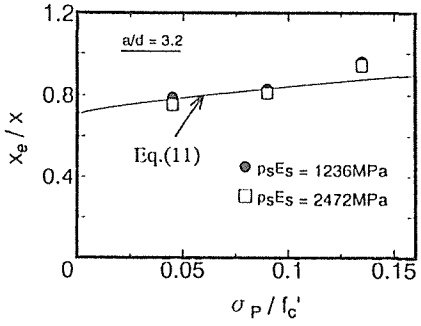

(b) For different stiffnesses of tendon

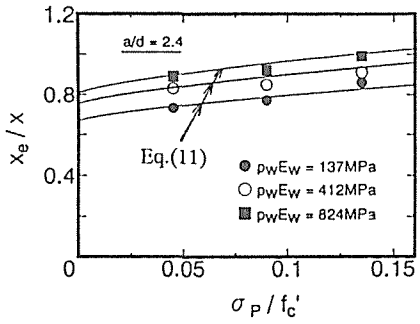

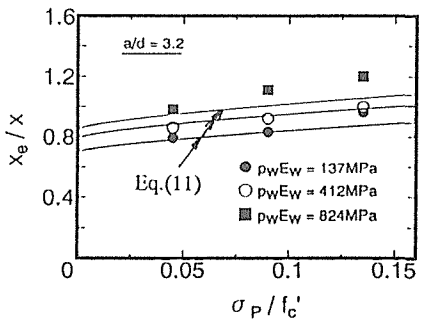

(c) For different stiffnesses of web reinforcement

Fig. 13 Relationships between Size of Compression Zone and Prestress Level

3. 3 Average Shear Stress at Compression Zone

Figure 14 shows relationships between the average principal stresses and a/d in the reinforced concrete beams. On the other hand, Fig.15 shows relationships between the average principal stresses and the prestress level in the prestressed concrete beams. In both the cases, the average of the minimum principal stress and the maximum principal stress are 0.80 and 0.15 times as large as concrete strength respectively. It was observed that these values were not dependent on the stiffness of the main and shear reinforcement. Therefore the failure criteria at the compression zone is defined as follows.

$$\frac{\overline{\sigma'_{2u}}}{f_c'}=0.80 \tag{12}$$

$$\frac{\overline{\sigma'_{1u}}}{f_c'}=0.15 \tag{13}$$

But the angle of the principal stress changes for different a/d ratios. Figure 16 shows relationships between the angle of the principal stress at the compression zone and a/d in the reinforced concrete beams. It is clearly seen that the angle becomes larger as a/d decreases. The angle was not depend on the concrete strength, the stiffness of main and shear reinforcement and the prestress level (see Fig. 17). So the angle is assumed as a function of a/d as follows.

$$\alpha = tan^{-1}\left(\frac{a}{d}\right)^{-1} \qquad (deg) \tag{14}$$

It can be said that solid lines in Figures 16 and 17 representing results predicted by Eq.(14) can predict the analyzed results well. The shear stress at the compression zone is a shear stress component of the principal stresses given in Eqs.(12) and (13).

$$\frac{\overline{\tau_{cpz}}}{f_c'} = 0.65 \sin\alpha \cos\alpha \tag{15}$$

Figure 18 shows relationships between the average shear stress normalized by the concrete strength and a/d in the reinforced concrete beams and Fig.19 shows relationships between the normalized average shear stress and the prestress level in the prestressed concrete beams. The predicted results shown by the solid lines are in good agreement with the analyzed results.

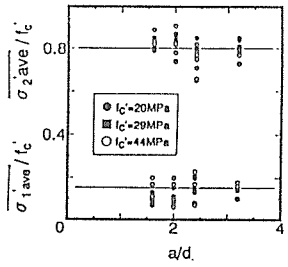

Fig. 14 Relationships between Average Principal Streses and a/d

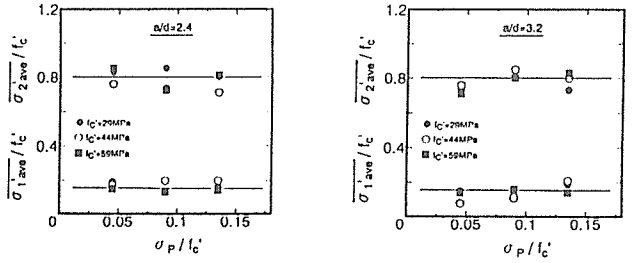

Fig. 15 Relationships betweer Average Principal Stresses and Prestress Level

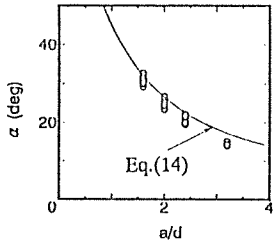

Fig. 16 Relationships between Angle of Principal Stress and a/d

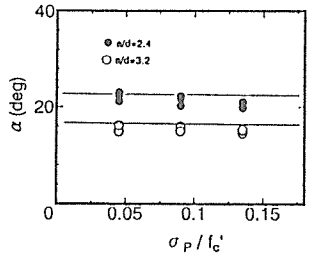

Fig. 17 Relationships between Angle of Prinhipal Stress and Prestress Level

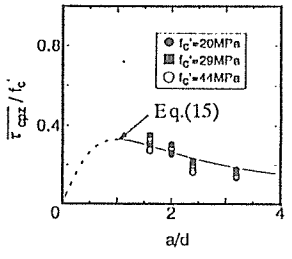

Fig. 18 Relationships between Average Shear Stress and a/d

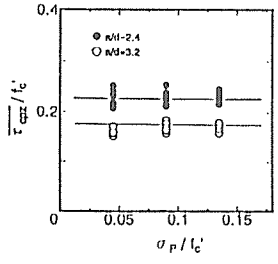

Fig. 19 Relationships between Average Shear Stress and Prestress Level

3.4 Average Compressive Stress at Horizontal Zone

Figure 20 shows relationships between the average of the maximum principal stress and the average of the minimum principal stress at the horizontal zone in the reinforced concrete beams. It can be considered that the horizontal zone is under uniaxial compressive stress state since the average of the maximum principal stress at the horizontal zone is only 10% of the minimum principal stress. The average of the principal stress did not depend on the stiffness of the main and web reinforcement. The same tendency was observed in the case of the prestressed concrete beams. Therefore the average compressive stress is assumed as a function of a/d and concrete strength only.

$$\frac{\overline{\sigma_2'_{ave}}}{f_c'}=0.64\left(\frac{a}{d}\right)^{-1} \tag{16}$$

Equation (16) can predict the analyzed results with a good accuracy as shown in Figs. 21 and 22. Figure 23 shows relationships between the angle of the principal stress and a/d in the reinforced concrete beams. It can be considered that the angles are the same for different a/d ratios. On the other hand the angle in the prestressed concrete beams is not the same. As shown in Fig.24 the angle of the principal stress decreases as the prestress level increases. It was observed, however, that the angle did not depend on the other parameters in both the cases. The angle of the principal stress at the horizontal zone is defined as a function of the prestress level as follows.

$$\beta=32\left[1-\left(\frac{\sigma_p}{f_c'}\right)^{0.5}\right] \qquad (deg) \tag{17}$$

The solid lines shown in Figs.23 and 24 represent the results predicted by Eq.(17). The average compressive stress at the horizontal zone is defined as a normal component of the principal stress given in Eq.(15) as follows.

$$\frac{\overline{\sigma'_{com}}}{f_c'}=0.64\left(\frac{a}{d}\right)^{-1}sin^2\beta \tag{18}$$

A dotted line shown in Fig.21 and a solid line shown in Fig.25 are the prediction of Eq.(18) in the case of the reinforced concrete and prestressed concrete beams respectively. From these figures, it is clearly seen that the results calculated by Eq.(18) are in good agreement with the analyzed results.

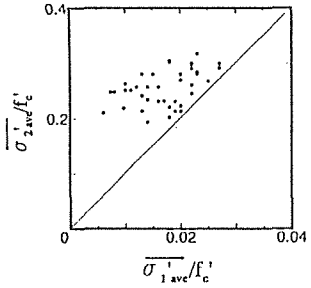

Fig. 20 Average Principal Stresses at Horizontal Zone

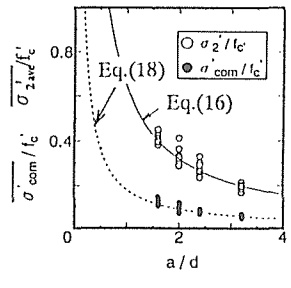

Fig. 21 Relationships between Average Stresses at Horizontal Zone and a/d

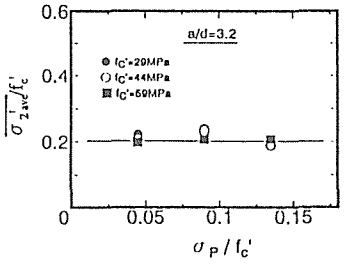

Fig. 22 Relationships between Average Stress at Horizontal Zone and Prestress Level

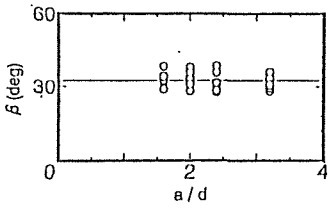

Fig. 23 Relationships between Angle of Principal Stress at Horizontal Zone and a/d

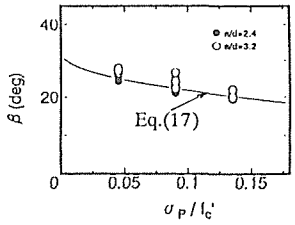

Fig. 24 Relationships between Angle of Prircipal Stress at Horizontal Zone and Prestress Level

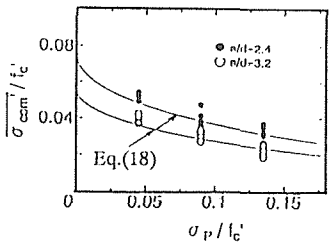

Fig. 25 Relationships between Average Compressive Stress and Prestress Level

3. 5 Average Shear Stress at Shear Cracking Zone

Figure 26 shows relationships between the average shear stress normalized by the 1/3 power of the concrete strength and a/d in the reinforced concrete beams. The effect of the concrete strength can be estimated by the 1/3 power of concrete strength. The figure also shows that shear stress becomes slightly larger as a/d increases. But the average shear stress does not depend on the stiffness of the main and web reinforcement (see Figs. 27 and 28).

On the other hand, the average shear stresses in prestressed concrete bemas become smaller than those in the reinforced concrete beams as the prestress level increases as shown in Fig. 29. Consequently, the following equation is assumed for prediction of the average shear stress at the shear cracking zone.

$$\frac{\overline{\tau_{str}}}{f_c'^{\frac{1}{3}}}=\frac{1.28}{\sqrt{a/d}+1}e^{-11.2\frac{\sigma_p}{f_c'}} \tag{19}$$

A solid line in each figure which shows the results predicted by Eq.(19) indicates that the predicted results agree well with the analyzed results in both the cases.

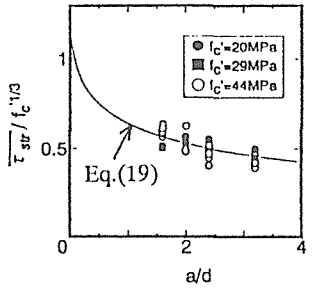

Fig. 26 Relationships between Average Shear Stress at Shear Cracking Zone and a/d

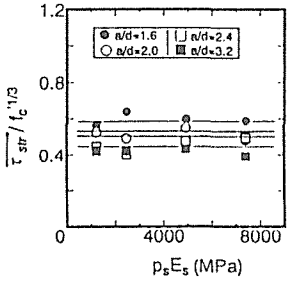

Fig. 27 Relationships between Average Shear Stress at Shear Cracking Zone and Stiffness of Main Reinforcemert

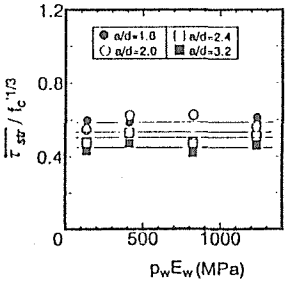

Fig. 28 Relationships between Average Shear Stress at Shear Cracking Zone and Stiffness of Web Reinforcement

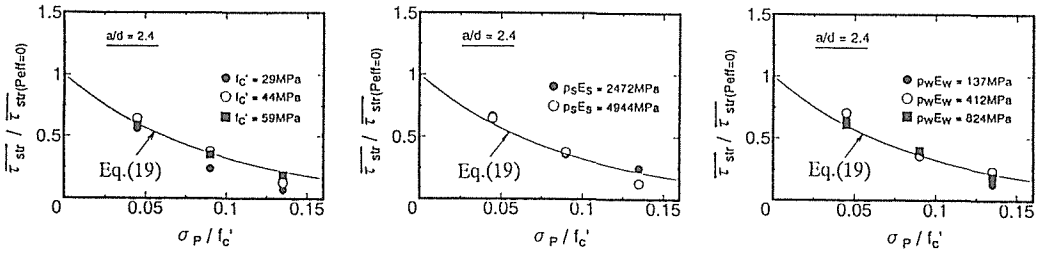

Fig. 29 Relationships between Average Stress at Shear Cracking Zone and Prestress Level

3. 6 Average Tensile Strain of Shear Reinforcement at Shear Cracking Zone

Figure 30 shows relationships between a/d and the average strain of the web reinforcement at the shear cracking zone at the ultimate stage of the reinforced concrete beams. The calculated strains increase as a/d decreases and the concrete strength increases. Figure 31 shows relationships between the stirrup strain and the stiffness of the main reinforcement. The average strain becomes larger when the stiffness of the main reinforcement becomes larger, but becomes smaller when the stiffness of the web reinforcement becomes larger as shown in Fig. 32.

On the other hand, the average stirrup strains in the prestressed concrete beams are slightly larger than those in the reinforced concrete beams as the prestress level increases as shown in Fig. 33. Judging from the above mentioned results, the following equation is presented in this study.

$$\overline{\varepsilon_{web}} = 0.0053 \frac{\sqrt{f_c'}}{\sqrt{a/d}+1} e^{\left(-\frac{1000}{p_s E_s} - 0.05\sqrt{p_s E_s}\right)} \left[1+\left(\frac{\sigma_P}{f_c'}\right)^{0.2}\right] \tag{20}$$

A solid line in each figure which is results predicted by Eq.(20) clearly indicates that Eq.(20) can predict the analyzed results.

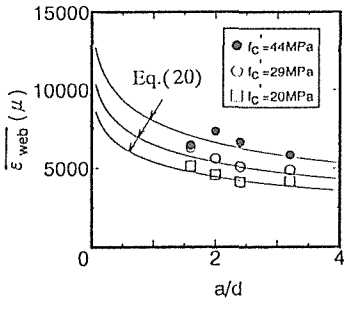

Fig. 30 Relationships between Average Stirrup Strain and a/d

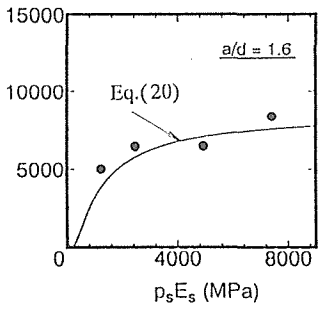

Fig. 31 Relationships between Average Stirrup Strain and Stiffness of Main Reinforcemert

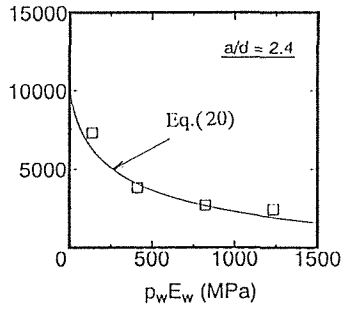

Fig. 32 Relationships between Average Stirrup Strain and Stiffness of Reinforcemert

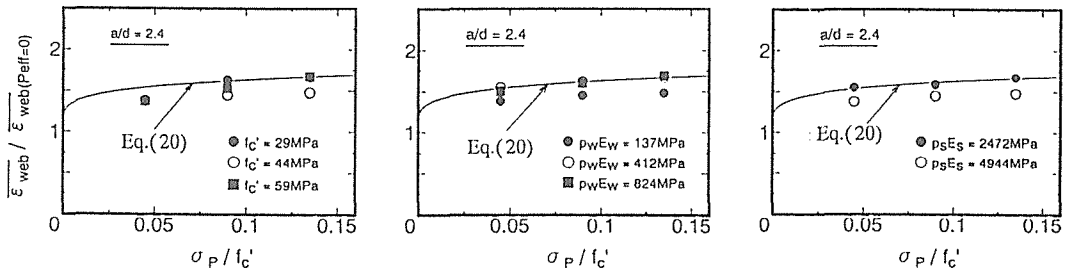

Fig. 33 Relationships between Average Stirrup Strain and Prestress Level

4. Shear Resisting Model in The Case Where Web Reinforcement Yields

The shear resisting model shown in Eqs.(3) and (4) is also assumed in the case where the web reinforcement yields. In this chapter, it will be discussed how to consider the yielding of web reinforcement in the shear resisting model for the case that web reinforcement does not yield.

The stiffness of the web reinforcement affects the depth of the compression zone and the average stirrup strain at the shear cracking zone. Figure 34 shows relationships between the average stirrup strain in the case where the web reinforcement does not yield. In this figure, a dotted line indicates the yield strain, ε_y of the web reinforcement. If the yield strain is lager than ε_i, beams fail before the web reinforcement yields. But if the yield strain is smaller than ε_i, the web reinforcement yields and the strain increases to point j (ε_j).

Figure 35 shows relationships between the stress and strain of the web reinforcement at the shear cracking zone in both the cases of steel bar and FRP rods at ultimate stage. If the steel strain and stress at ultimate stage will be given, an equivalent Young's modulus can be calculated by the following equation.

$$E_{w-e}=\frac{\overline{\sigma_s}}{\varepsilon_{web}} \tag{21}$$

where E_{w-e}: equivalent Young's modulus (see Fig. 35). In Fig. 34, the pass-A indicates the strain changing in case where the web reinforcement has an equivalent stiffness, $E_{w-e}p_w$. On the other hand, the stirrup strain increases since the stiffness of the web reinforcement decreases gradually when the strain reaches at the yielding point (pass-B). If the difference in the strain path does not affect the shear strength, it can be said that the shear strength of a beam in which the stiffness of the web reinforcement does not change (pass-A) is equal to that of a beam in which the stiffness of the web reinforcement decreases because of the yielding (path-B).

Figure 36 shows the shear force-deflection curves of the analyzed two specimens. One is the reinforced concrete beam with the stiffness of the web reinforcement of 412 MPa and the yielding strength of 300 MPa, and another is the reinforced concrete beam with the equivalent stiffness of 108 MP using the equivalent Young's modulus calculated by Eq.(21). It is observed that there is a small difference before the web reinforcement yields but good agreement at the ultimate stage. The shear strengths of the yielding case and no yielding case are 188 kN and 186 kN respectively.

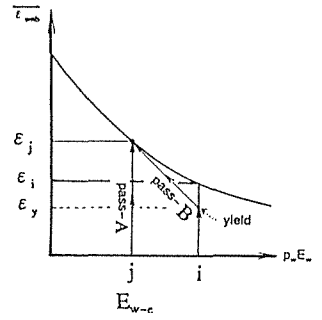

Fig. 34 Relationships between Average Stirrup Strain and Stiffness of Web Reinforcement

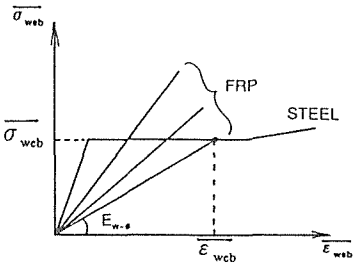

Fig. 35 Relationships between Stress and Strain at Shear Cracking Zone

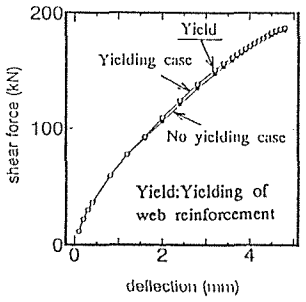

Fig. 36 Shear Force-Deflection Curves

5. Verification of Proposed Shear Resisting Model

5.1 Prediction of Shear Strength of Concrete Beams Reinforced with FRP Rods

Verification of the proposed shear resisting model will be conducted for the reported test data of reinforced and prestressed concrete beams reinforced with FRP rods (see Table 1)[5)-10)].

Figures 37 to 40 show relationships between ratio of the shear strengths (Experiment/Prediction) and a/d, the concrete strength, the stiffness of the main reinforcement, and the stiffness of the web reinforcement in the case of the reinforced concrete beams. From Figs. 37 and 38, no influence of the concrete strength nor a/d is observed. It is clearly seen that the shear strength ratio is smaller than 1.0 when the stiffness of the web reinforcement is less than 100 MPa. And the ratio becomes smaller as the stiffness of the main reinforcement decreases as shown in Fig. 39.

In beams which have a low stiffness of main and/or web reinforcement as well as beams without web reinforcement diagonal tension failure is caused by single cracking. However the finite element program used in this study cannot simulate exactly the diagonal tension failure. Therefore the proposed model developed by the numerical study using the program cannot be applied to the diagonal tension strength. The average of the shear strength ratios in the case where the stiffnesses of the web reinforcement were less than 100 MPa is 0.66 and the coefficients of variation is 17%. The average of the shear strength ratios in case where the stiffnesses of the web reinforcement were 100 MPa or more is 0.98 with the coefficient of variation of 18%. It can be said that the proposed model is applicable to concrete beams

with a stiffness of web reinforcement which is equal to or greater than the 100 MPa.

Figure 41 shows relationships between the shear strength ratio and the stiffness of the web reinforcement of the prestressed concrete beams reinforced with FRP rods. It seems that the proposed model underestimates the test results slightly. The average of the shear strength ratio is 1.18 and the coefficient of variation is 7.8%. It is generally known that failure mode is changed from the diagonal tension failure to the shear compression failure as a prestressing force increases. In fact, this tendency was observed in the experiment[8]. It can be said that the proposed model can be applied to prestressed concrete beams with a stiffness of web reinforcement which is even less than 100 MPa.

Table Test Specimens

	P_{ef} (kN)	a/d	f_c' (MPa)	p_sE_s (MPa)	p_wE_w (MPa)
Ref.5	-	3.1-3.2	39-42	1963-9574	48-242
Ref.6	-	2.4	38-41	2800-9826	297-493
Ref.7	-	2.5	30-38	518-1986	114-325
Ref.8	-	3.0	44-45	982	50-76
Ref.9	-	2.7	45	513	224-654
Ref.10	-	3.0	57-59	6588	116-274
Ref.11	123-179	3.0	38-60	982	56-107

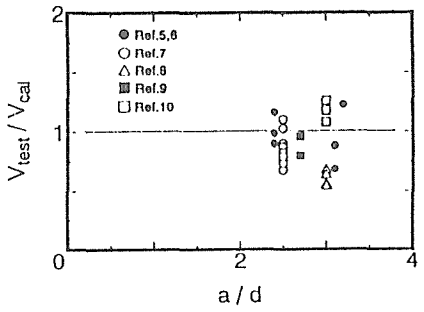

Fig. 38 Relationships between Shear Strength Ratio and a/d

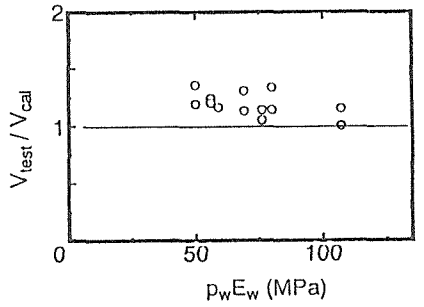

Fig. 40 Relationships between Shear Strength Ratio and Stiffness of Web Reinforcement

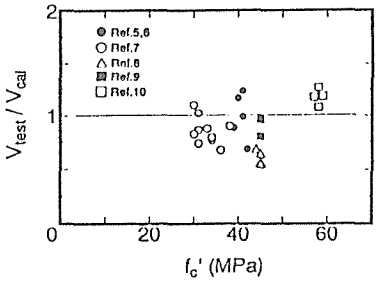

Fig. 37 Relationships between Shear Strength Ratio and Concrete Strength

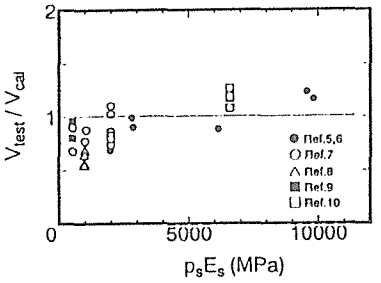

Fig. 39 Relationships between Shear Strength Ratio and Stiffness of Main Reinforcement

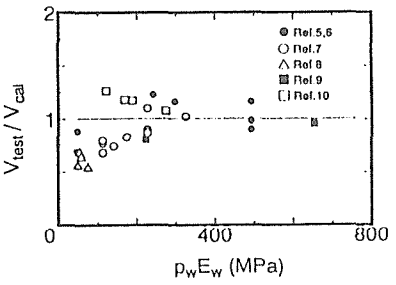

Fig. 41 Relationships between Shear Strength Ratio and Stiffness of Web Reinforcement

5. 2 Prediction of Shear Strength of Concrete Beams Reinforced with Steel

Verification of the proposed shear resisting model will be conducted also for the reported test data of reinforced and prestressed concrete beams reinforced with steel bars (see Table 2)[11)12)13)].

Figure 42 shows relationships between the shear strength ratio and the concrete strength. Although the proposed model overestimates the test results slightly for the case of concrete strength of about 90MPa and underestimates for the case of concrete strength of about 10 MPa, it can be said that the calculated results are in agreement with the test results generally. The specimens with the concrete strength of about 10 MPa are deep beams. Figure 43 shows relationships between the shear strength ratio and a/d. It is clearly seen that the proposed model can predict the shear strengths of beams in which a/d is greater than 1.5. The proposed model is developed under the condition that a shear span(a) is greater than its height(h), that is, $a/h>1.0$ (see Eq.(5)). The average of the shear strength ratio for the case of a/d smaller than 1.5 is 1.62 with the coefficient of variation of 28%. The average of shear strength ratio for the case of a/d equal to more than 1.5 is 1.07 with the coefficient of variation of 13%. From Fig .44, no influence of the web reinforcement ratio is observed.

Figure 45 shows relationships between the shear strength ratio and the prestress. It is seen that the predicted results are in good agreement with the experimental ones. The average of the shear strength ratio of the prestressed concrete beams is 1.03 and the coefficient of variation is 13%.

Table 2 Test Specimens

	P_{eff} (kN)	a/d	f_c' (MPa)	p_s (%)	p_w (%)	f_{wy} (MPa)
Ref.12	-	3.6	24-90	3.36	0.11-0.36	269-323
Ref.13	-	0.5-2.0	17-25	2.46	0.29-1.20	341-400
Ref.14	41-134	1.7-4.2	20-70	1.05-2.22	0.21-0.43	235-529

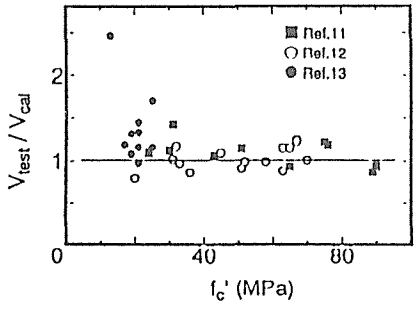

Fig. 42 Relationships between Shear Strength Ratio and Concrete Strength

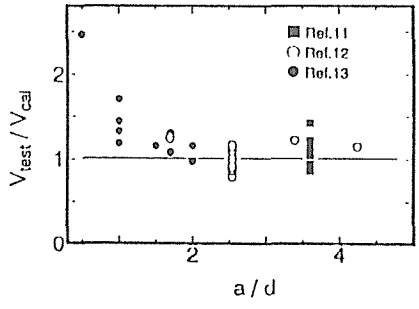

Fig. 43 Relationships between Shear Strength Ratio and a/d

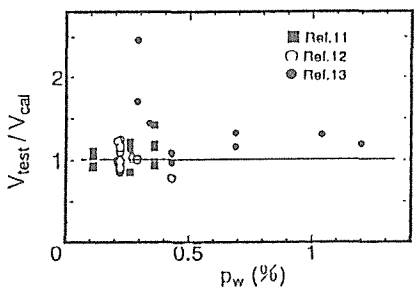

Fig. 44 Relationships between Shear Strength Ratio and Web Reinforcement

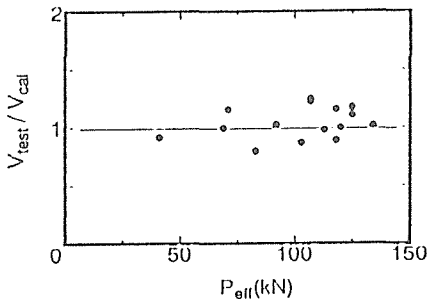

Fig. 45 Relationships between Shear Strength Ratio and Prestressing Force

6. Conclusions

(1) A shear resisting model for beams was developed by numerical study using nonlinear finite element analysis. The model can be applied to non-prestressed and prestressed concrete beams reinforced with FRP rods and/or steel bars. The shear resisting model is defined as a summation of shear resisting forces carried by concrete at compression zone, by web reinforcement and others at shear cracking zone, and by concrete at horizontal zone linking the compression and shear cracking zones.

(2) It was confirmed that the proposed shear resisting model can predict the shear strengths of reinforced concrete beams and prestressed concrete beams accurately.

Acknowledgments

We would like to thank Dr.Nares Pantaratorn who developed the program used in this study.

References

1) For example, K. Sakai, T. Okosi, T. Minematsu and K. Kawamata : Application of Cathodic Protection to RC Structures in Cold and Snowy Region, Proc. of the JCI, Vol. 13, No. 1, pp. 567-572, June 1991 (in Japanese).

2) Y. Sato, T. Ueda and Y. Kakuta : Qualitative Evaluation of Shear Resisting Behavior of Concrete Beams Reinforced with FRP Rods by Finite Element Analysis, Proc. of JSCE, Vol. 22, No. 484, pp. 51-60, February 1994 (in Japanese).

3) N. Pantaratorn : Finite Element Analysis on Shear Resisting Mechanism of RC Beam, Dissertation Submitted to the University of Tokyo, March 1991.

4) J. Niwa : Equation for Shear Strength of Reinforced Concrete Deep Beams Based on FEM Analysis, JCI-C5, pp. 119-128, October 1983 (in Japanese).

5) Y. Sato, N. Wada, T. Ueda and Y. Kakuta : Shear Resisting Mechanism of RC Beams Using FRP Rods by Finite Element Analysis, Proc. of JSCE Symposium on Concerning Application to the Field of Civil Engineering Structures of Concrete Based Composite Material Using Continuous Fibers, pp. 173-180, April 1992 (in Japanese).

6) K. Nishizono, Y. Sato, Y. Takahashi, T. Ueda and Y. Kakuta : Shear Behavior of Concrete Beams Reinforced with FRP Rods by Laser Speckle Method, Proc. of JSCE Hokkaido Branch, Vol. 49, pp. 963-

966, February 1993 (in Japanese).
7) S. Kanekura, K. Maruyama, K. Shimizu and Y. Nakamura : Shear Behavior of Concrete Beams Reinforced by CFRP Rods, Proc. of JCI, Vol. 15, No. 2, pp. 887-892, June 1993 (in Japanese).
8) H. Wakui and S. Tottori : Reinforcing Effect of Spiral FRP Rods as Shear Reinforcement, Proc. of JCI, Vol. 12, No. 2, pp. 1141-1146, June 1990.
9) T. Honda, H. Ikeda and T. Tachibanada : A Study on Shear Property of Concrete Members Reinforced with FRP Stirrups, Proc. of the 45th Annual Conference of the JSCE, September 1990 (in Japanese).
10) K. Okumura, Y. Murayama, R. Amano and B. Bujadham : Effect of Characteristic of Reinforcement to Tensile Stiffness of Concrete Members, Proc. of JSCE Symposium on Concerning Application to the Field of Civil Engineering Structures of Concrete Based Composite Material Using Continuous Fibers, pp. 173-180, April 1992 (in Japanese).
11) A. G. Mahone and G. C. Frantz : Shear Tests of High and Low Strength Concrete Beams with Stirrups, SP-87, ACI, pp. 179-196, 1985.
12) T. Hayashikawa, F. Saitoh and Y. Kakuta : Strength of Reinforced Concrete Deep Beams with Shear Reinforcement, Proc. of the JCI, Vol. 12, No. 2, pp. 319-324, June 1990 (in Japanese).
13) K. Cederwall, O. Hedman and A. Loeberg : Shear Strength of Partially Prestressed Beams with Pretentioned Reinforcement of High Grade Deformed Bars, SP-49, pp. 218-230, 1974.